GUANGZHONG SUN
RUNLIN ZHANG
and
KUNYUN TIAN

Experimental study of the evolution of permeability in coal containing gas during short-term creep under multi-stage loading

Aiming at understanding the evolution characteristics of permeability in coal masses containing gas during creep, samples of coal containing gas were collected from the No. 3 coal seam of Rundong coal mine, Yangcheng, China for analysis. The seepage is tested during the creep process in multi-stage axial load apparatus under different confining pressures using a self-developed multi-stage triaxial stress loading device allowing analysis of seepage during creep processes. Experimental results shows that: (1) obvious attenuation creep deformation and static deformation appeared during the creep process caused by multi-stage loading under low stresses, and the permeability decreased during the loading process and creep stage. The permeability decreased at a high rate in the initial stages of testing, gradually reaching a stable value and, it changed in the opposite sense to the axial deformation. Moreover, high confining pressures had certain inhibiting effects on the change in permeability of the coal samples; (2) The permeability varied slightly in the attenuated, and steady, stages under the failure stress of creep, and it decreased in the attenuated stage, while it linearly increased under steady state conditions. In the accelerated stage, the permeability increases significantly and it is several times greater than the initial permeability in the steady creep stage when the coal body is damaged; (3) In the creep damage stage, the changes in the permeability and volumetric strain conformed to an exponential function.

Keywords: *Short-term creep, seepage, tectonic coal, multi-stage loading, permeability.*

1. Introduction

Coal, as a porous medium, has creep mechanical properties and changes in its seepage field as key mechanical properties. Aiming at research into the coupling of creep and seepage in porous media, Xu Jiang et al. [1] carried out a seepage experiment during creep under triaxial stress loading of coal samples, and obtained a trend in the permeability evolution of coal samples under different temperatures and effective stress levels. Yin Guangzhi et al. [2] studied the creep properties of coal under different confining pressures and gas pressures by performing seepage experiments during creep under triaxial stress states. In addition, the creep properties were analysed theoretically in conjunction with a seven-component Hohai model. Wang Dengke et al. [3] analysed the creep properties of coal samples under different creep conditions, confining pressures, and gas pressures by using aself-developed triaxial creep test system. In addition, they studied creep rates in the attenuated stage and under steady state creep processes and proposed a formula for the calculation of creep rates. He Feng et al. [4] acquired a relationship linking creep deformation and permeability and revealed the consistency of the permeability evolution and creep damage based on experimental investigations of seepage in coal and rocks during creep. Wang Rubin et al. [5] carried out a creep test on metamorphic volcanic breccia to analyse creep deformation properties under different stresses and examined the changes in the permeability during creep. Aiming at understanding the dynamic changes in various physical parameters such as porosity and permeability under creep in a rock mass, Wei Jia et al. [6] deduced a fluid-solid coupling calculation model under creep conditions. Guo Baohua et al. [7] discussed the normal creep deformation of rock fractures and the influence of seepage through experimental work. Cao Yajun et al. [8] analysed the evolution of the permeability of monzonitic granite under multi-stage loading during creep processes through experiments. Aiming at understanding the influences of fractured rock mass joint and fissure closures on permeability, Chen Junguo et al. [9] established a fluid-solid coupling model to ascertain the influences of extent of fracturing of the rocks on their permeability under creep load through numerical analysis. Aiming at knowledge of the seepage properties of sandstones during creep processes, Dai Zhixu et al. [10] conducted an experiment to obtain the

Messrs. Guangzhong Sun, Runlin Zhang and Kunyun Tian, School of Safety Engineering, Henan Institute Engineering, Zhengzhou, Henan 451 191, Guangzhong Sun, School of Resources and Safety Engineering, Central South University, Changsha, Hunan and Guangzhong Sun, Runlin Zhang and Kunyun Tian, Key Laboratory of Coal Mine Safety Training in Henan Province, Zhengzhou, Henan 451 191, China. E-mail: sgz228165@126.com

relationship between rock stress states and pore-water pressure with seepage coefficients. Zhang Yu et al. [11] analysed permeability evolution during stress-strain processes and studied the evolution of seepage coefficients during creep by conducting experiments on seepage in sandstones with poor integrity of the fractured zones therein. Yang Hongwei et al. [12] studied creep properties during creep in a multi-stage triaxial test under hydraulic pressure: by doing so, they analysed the creep properties of rocks and the changes in permeability coefficients under different hydraulic pressures.

For the excavation of underground coal and rocks, the load and surrounding rock stress change with changes in construction or mining activities. Creep, in coal and rocks under progressive load, is an important physico-mechanical effect: progressive loading is also a common experimental method for creep deformation assessment of coal and rocks. Therefore, it exerts an important theoretical and practical influence warranting this study of seepage properties in different stages of coal creep under multi-stage loading.

2. Experimental principles and methods

2.1 Test coal samples and equipment

Coal samples were collected from the No.3 coal seam of Jinsheng-Rundong Coal Mine, Yangcheng, Shanxi Coal Group in China. The coal was composed of moisture (Mad) 1.92%, an ash content (Ad) of 15.1%, volatiles (Vdaf) to 7.8%, and fixed carbon (Fcd) to 75.18%. According to the standards of GB/T50266-2013 and ISRM, standard cylindrical samples were prepared measuring 50 mm (diameter) × 100 mm (height) (Fig.1).

Fig.1 Coal samples

The experiment was conducted on an automatic triaxial seepage experimental testing system for coal and rock samples. Modified based on triaxial fracturing test equipment [13], the instrument was endowed with functions enabling it to automatically collect, and record, data. In addition, confining pressures and axial loadings can be tracked, and it was able to achieve constant loading for a long time. The instrument can apply load in three ways, including stress, strain, and flow control (Fig.2).

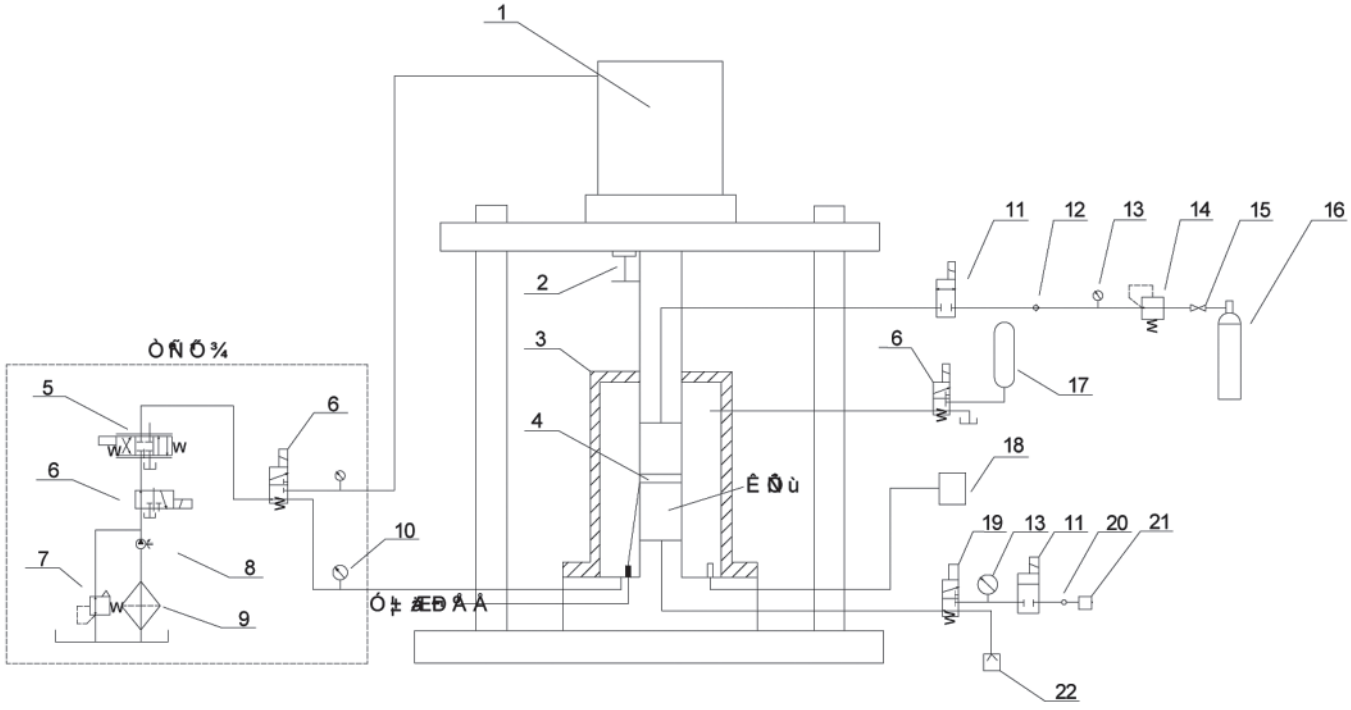

1. Hydraulic cylinder; 2. Extensometer; 3. Triaxialcell 4.Strain gauge; 5. Servo-valve; 6. Two-position three-port directional control valve; 7. Overflow valve; 8.Hydraulic pump; 9. Filter; 10. Pressure gauge; 11. Two-position three-port magnetic valve; 12. One-way valve; 13. Barometer; 14.Reducing valve; 15. Ball valve; 16. Air storage tank; 17. Energy accumulator; 18. Temperature controller; 19. Magnetic valve (two-position three-way); 20. Flowmeter; 21.Exhaust port; 22. Vacuum pump

Fig.2 Principle of the triaxial creep-seepage servo-test system

2.2 Experimental principles

To analyse and measure the changes in permeability of the coal samples, it is assumed that initial pores and microcracks were uniformly distributed therein and the samples could therefore be regarded as porous. In addition, steady seepage under constant pressure was considered continuously, and conforming to Darcy's law. Experiments measuring the permeability were conducted by using the steady state method. After imposing axial loads and confining pressures on a coal sample, scheduled gas pressures were steadily imposed on the upper end of the sample via the reducing valve. The other end of the sample was subjected to negative pressures by applying the vacuum pump to maintain the pressure difference between the two ends for a certain time. CH_4, with a purity of 99.9%, was used as the seepage medium. Due to the adsorption of methane gas on the coal matrix, the adsorption equilibrium of gas was evaluated and then axial loading applied only when steady seepage was established. Next, axial loads and the confining pressure were kept unchanged to conduct the experiment on gas seepage during short-term creep by using the tracking pump for axial loads and confining pressures. It can be seen from the experimental principle that the permeability of the coal samples was calculated by using Darcy s law:

$$k = \frac{2\mu p_0 Q_0 L}{[p_1^2 - (p_0 - p_2)^2]S} \quad \ldots \quad (1)$$

where, μ, p_0 and Q_0 represent the coefficient of kinetic viscosity of the gas (Pa·s), standard atmospheric pressure (Pa), and the seepage flow under standard atmospheric pressure (cm^3/s), respectively, and L, p_1, p_2 and S represent the length of the samples (cm), input gas pressure on the upper end face of the samples (Pa), negative outlet pressure on the bottom end face of the samples (Pa), and the cross-sectional area of the coal samples (cm^2), respectively.

2.3 Experimental procedure

Temperature changes were not taken into account during testing. The temperature of the laboratory was kept constant by employing constant-temperature air-conditioning. Before conducting creep deformation experiments, the air-tightness of the coal and rock samples was tested. The test procedures for seepage evaluation of coal samples in triaxial compression during creep processes were as follows:

(1) According to test requirements, a strain gauge was pasted onto the side surfaces of each coal sample. Then gel was smeared onto the side surfaces of the coal sample and smoothed off. Then, heat-shrink tubing was applied to the coal sample under test. Next, the space between the heat-shrink tubing and the side surface of the sample was eliminated by using a blower and the pressure head was brought into full contact with the top and bottom surfaces of the sample. It was connected to both the inlet and outlet of the gas on the top and bottom of the sample and then the data collection system was started. In addition, in order that methane gas was the only gaseous phase in the coal sample, the bottom of the coal sample was placed under vacuum for at least 8h.

(2) Axial and lateral pressures were imposed as the confining pressure, which was determined by experimental schemes from the outset. Confining pressures were kept equal to the applied axial pressure. After the confining pressure was stabilised, gas pressures and negative loads were imposed on the upper plane and the lower plane of the sample, respectively. This ensured that confining pressure was larger than the pore pressure to avoid over-large gas pressures fracturing the heat-shrink tubing. During the experiment, the stress system was kept at constant pressure to force the gas to be adsorbed on the coal sample for 12h.

(3) The axial stress loading cycles were performed and creep stress (first stage) was slowly imposed to its predetermined value at a rate of 0.5 MPa/min. Then various parameters were kept unchanged (i.e., the axial pressure, confining pressure, and gas pressure. The creep loading was progressively imposed until accelerated damage appeared under final-stage loading according to the changes in strains.

The test plan is listed in Table 1.

Table 1: Test plan: triaxial creep experiments

Sample number	Confining stress/MPa	Gas pressure /MPa	Negative pressure/kPa
1-1	2	1.0	20
1-2	4	1.0	20
1-3	6	1.6	20
1-4	8	1.0	20

3. Experimental results

Through various effects imposed on the coal samples including different confining pressures, gas pressure on the upper surface and negative pressure on the lower surface, the permeability test was conducted to progressively increase axial pressures until accelerated creep damage appeared. The test result is displayed in Fig.3: the creep process of the sample displays different features under different axial pressures. The creep deformation gradually increased during the entire process, and the permeability linearly declined on the whole under lower axial stresses while it dramatically increased under creep failure stresses. It can be seen from the experiment that the change in the permeability of the coal samples was uniform under different confining pressures and gas pore pressures.

4. Evolution of permeability in coal samples under creep

4.1 Evolution of permeability in coal samples under low-stress levels

Fig.4 shows the permeability evolution of coal samples

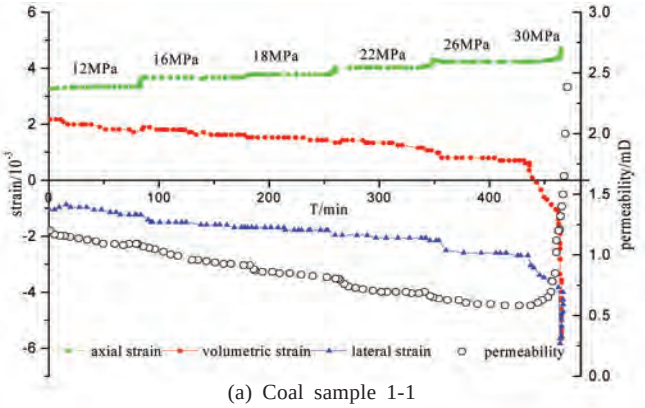

(a) Coal sample 1-1

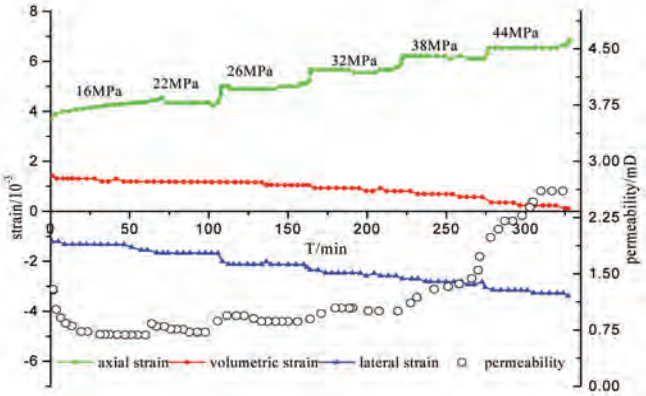

(b) Coal sample 1-2

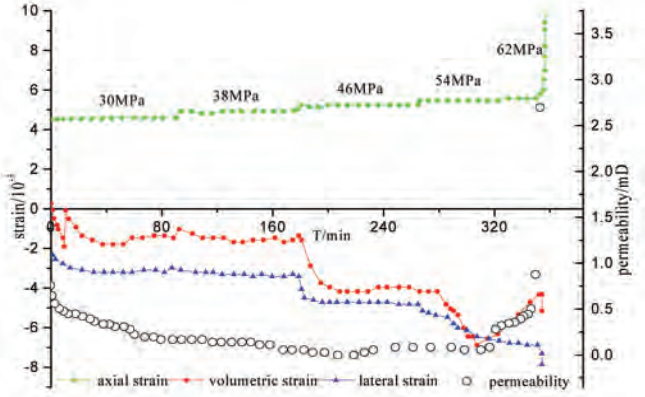

(c) Coal sample 1-3

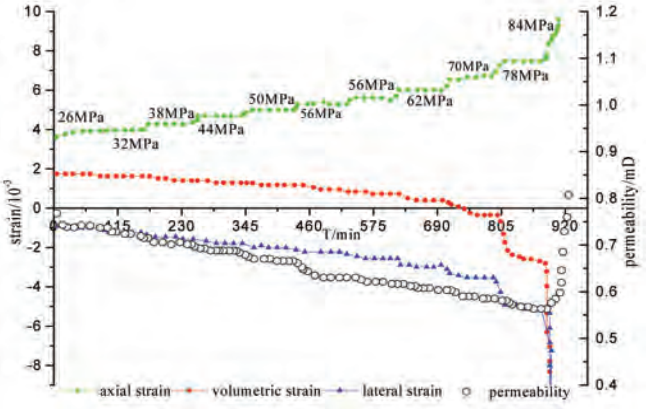

(d) Coal sample 1-4

Fig.3 Evolution of permeability in coal samples during creep testing

under initial stress application. The first-stage loading on the coal sample was 60% of their instantaneous strength during initial loading. As the strength of the coal samples increased with increasing confining pressures, non-uniform first-stage axial loadings were imposed on the coal samples under different confining pressures. According to previous experiments, it can be found that the uniaxial compressive strength of experimental samples is about 20 MPa, so the first-stage loads imposed on coal samples 1-1, 1-2, 1-3, and 1-4 were 12, 16, 30, and 26 MPa, respectively.

Fig.4 shows that the permeabilities of the samples all decreased with time. Permeability reduced at a high rate in the initial stage, gradually reaching a stable value. While the axial deformation changed in the opposite sense to the permeability: it gradually increased with time and finally reached a stable value. This was because deformation of the coal samples gradually entered an attenuated stage of the creep process with the application and stabilisation of the first-stage load. In addition, the coal sample was under triaxial compression due to the effects of axial pressure and confining pressure. Under such conditions, fractures were gradually closed and seepage passages became narrow or were blocked while the gas seepage flows gradually declined so that the permeability decreased. Deformation of the coal samples increased while the growth rate tended to zero with the transformation from the attenuated stage to stable creep. At this time, no fractures appeared in the coal samples. It can be seen from the experimental data that the permeabilities of the coal samples reduced under this condition and were basically stabilised.

It can be seen from initial values of the permeability that initial permeabilities of coal samples 1-1, 1-2, 1-3, and 1-4 were 1.202, 1.292, 0.758 and 0.767 mD, respectively. Low confining pressures exhibited a minimum closure effect on rock fractures, so the permeabilities of coal samples 1-1 and 1-2 were around 1.5 times those of 1-3 and 1-4. The initial permeability of coal sample 1-3 under a gas pressure of 1.6 MPa was almost the same as that of sample 1-4 under a gas pressure of 1 MPa, so the pore pressures exerted an insignificant influence on the permeability. In addition, the permeability of coal sample 1-1 was almost the same as that of 1-2, and the permeability of coal sample 1-3 differed only slightly from that of 1-4. This was mainly because gas seepage passages were controlled by effective stress while the two pairs showed almost the same effective stresses. In addition, pores and fractures in the coal samples were compressed under effective stress, causing parts of the effective passages for gas seepage to be blocked and therefore the permeability decreased.

4.2 Evolution of permeability of coal samples under failure stress

Accelerated creep occurred in the coal samples under different confining pressures with the increase of axial stress,

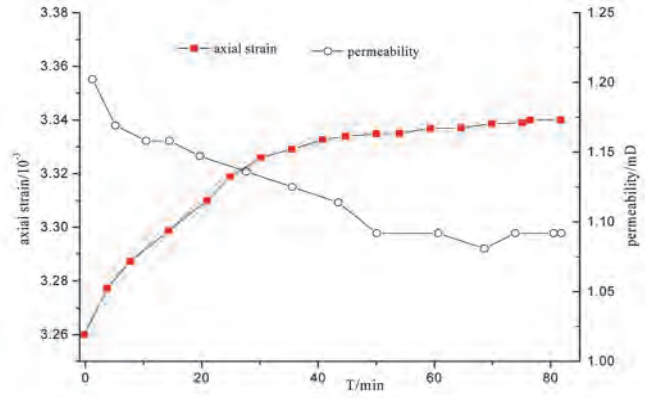

(a) Axial stress, 12 MPa, confiningpressure, 2 MPa, and gas pressure, 1 MPa

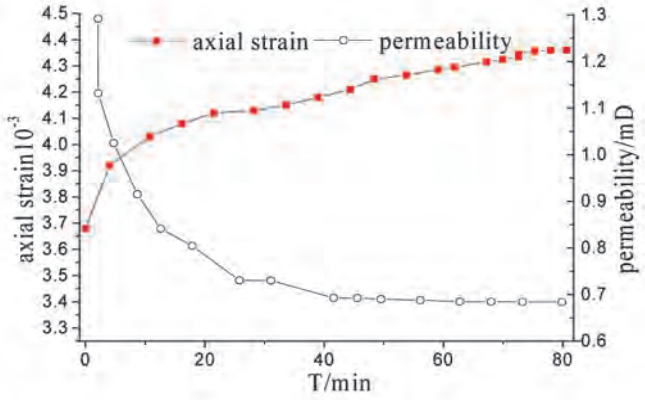

(b) Axial stress, 16 MPa, confining pressure, 4 MPa, and gas pressure, 1 MPa

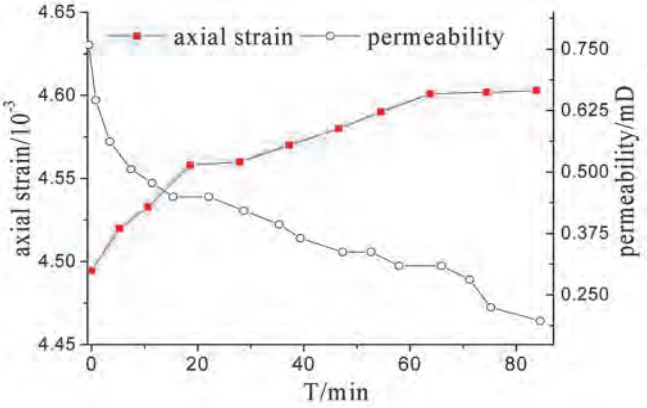

(c) Axial stress, 30 MPa, confining pressure, 6 MPa, and gas pressure, 1.6 MPa

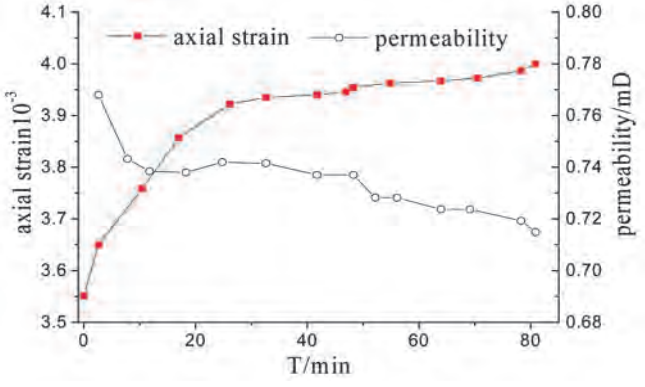

(d) Axial stress, 26 MPa, confining pressure, 8 MPa, and gas pressure, 1 MPa

Fig.4 Evolution of permeability under initial stress

which significantly differed from the coal deformation and permeability evolution under low stress when analysing the permeability evolution of the coal samples. The coal samples showed two-stage deformation under low stress including instantaneous deformation and steady creep. Under such stresses, because the coal samples were in a triaxial stress state, pores and fractures inside were compressed and the samples presented insignificant changes in their internal structures. The structural change was illustrated by the linearly decreasing permeability, which was, on the whole, a relatively stable process. While, pores and fractures inside the coal samples were further damaged under failure stresses so that new cracks appeared and the intersection of multiple cracks formed effective gas passages, which was conducive to gas transport within the coal samples. Fig.9 shows that remarkable shear characteristics appeared in coal samples at their failure state and obvious connected fractures occurred in the axial direction, which was the primary reason for the sudden change in permeability. Fig.5 shows the relationship between permeability and time when the axial stress reached the failure level of the coal samples under different gas stresses and confining stresses. Loading via axial stress exerted a compressive effect on the coal samples under this failure stress, resulting in a reduction in their permeability from the outset. It can be seen from the data that the permeability evolution lagged the applied stress: as it continued, the creep could be divided into three stages under axial failure stress: attenuated creep, steady creep, and accelerated damage. In the first two stages, the permeability did not change significantly but gradually increased with time. This was because micro-fractures gradually formed in the coal samples and widened slowly. Damage to the coal samples further increased upon entering the accelerated creep stage, as shown by the increase in creep rate from a deformation perspective. In addition, the volume of the coal samples increased (showing an obvious dilatation) and the fractures widened further. As a result, fractures inside the coal samples were connected to form effective passages for gas seepage, as illustrated by the sudden linear increase in coal permeability when viewed macroscopically. It can be seen from the permeability evolution in the coal samples that the permeability of damaged coal samples grew rapidly with time while the later permeability evolution was not measured here.

Figs. 6 to 8 show the creep properties and permeability evolution of the coal samples in the three stages under axial failure loads. Table 2 lists the permeabilities during the three stages under failure stress and creep conditions. Experimental results show that, from the first two stages to the accelerated failure stage, the initial values of permeability in the failure stage were 1.30, 1.61, and 1.006 times those in the attenuated creep stage, respectively. In addition, a comparison showed that the initial values in the steady creep stage were 1.34, 7.24, and 1.03 times as large as the original permeability. From the coal sample under a confining pressure of 8 MPa, it can be

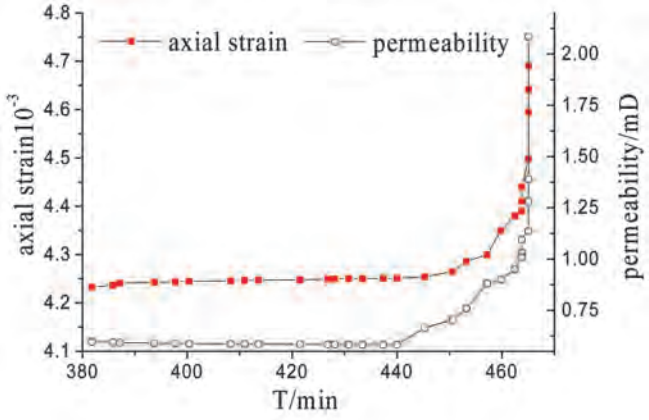

(a) Axial stress, 30 MPa, confining pressure, 2 MPa, and gas pressure, 1 MPa

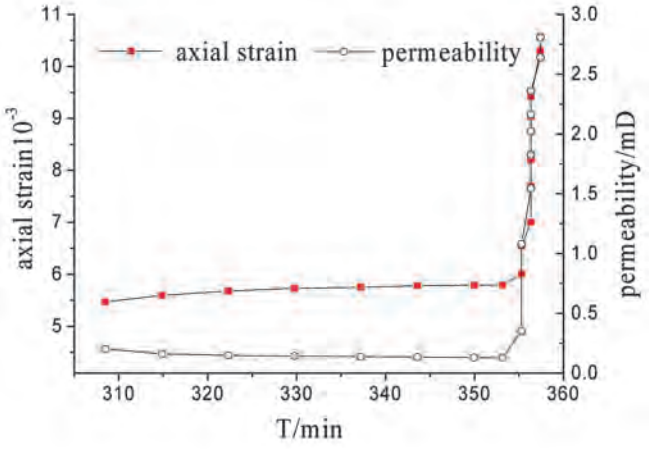

(b) Axial stress, 62 MPa, confining pressure, 6 MPa, and gas pressure, 1.6 MPa

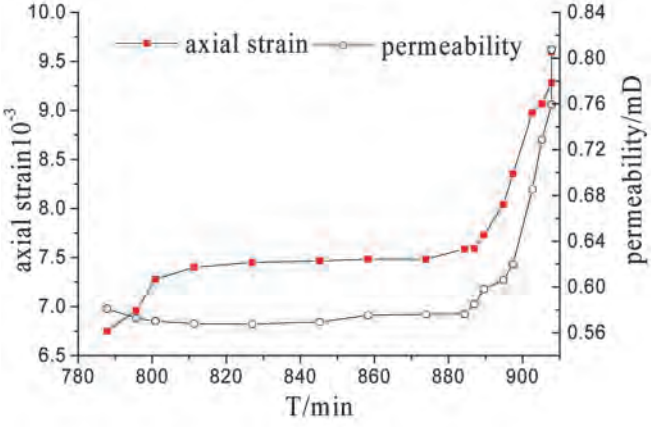

(c) Axial stress, 84 MPa, confining pressure, 8 MPa, and gas pressure, 1 MPa

Fig.5 Evolution of permeability at failure

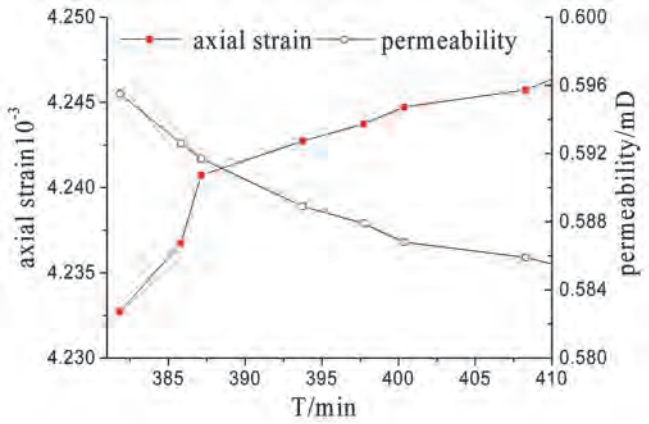

(a) Confining pressure, 2 MPa and gas pressure, 1 MPa

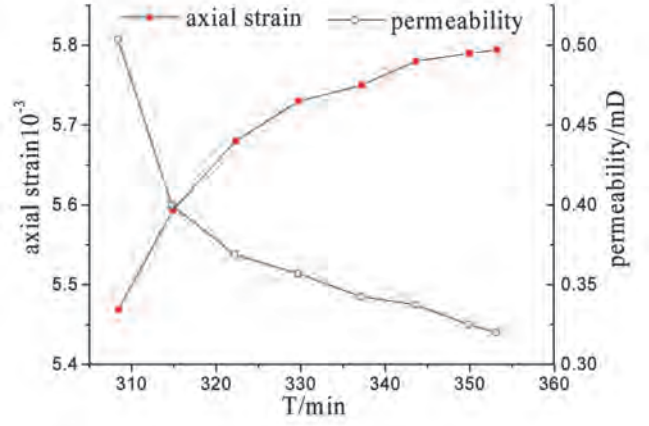

(b) Confining pressure, 8 MPa and gas pressure, 1 MPa

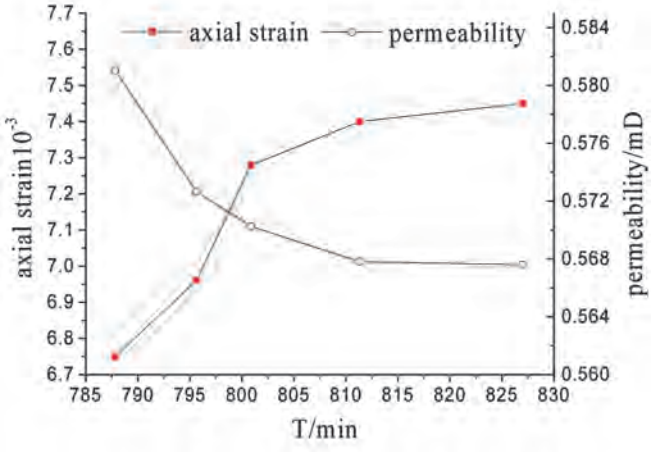

(c) Confining pressure, 8 MPa and gas pressure, 1 MPa

Fig.6 Evolution of permeability in the attenuated creep stage under failure stresses

seen that the permeability increased but only insignificantly: this was because final-stage creep load was large so the permeability changed with less sensitivity to stress as the coal samples were under compression as a result of the imposed effective stresses. The permeabilities of the coal samples after failure were significantly larger than those in the first two stages. In addition, the initial permeabilities at the start of the failure stage were 4.37, 5.57, and 1.38 times as large as those in the attenuated creep stage.

Fig.9 shows the failure state of the coal masses containing gas during multi-stage loading under creep conditions. The coal samples mainly presented shear failures and showed apparent dilatational characteristics during failure with the

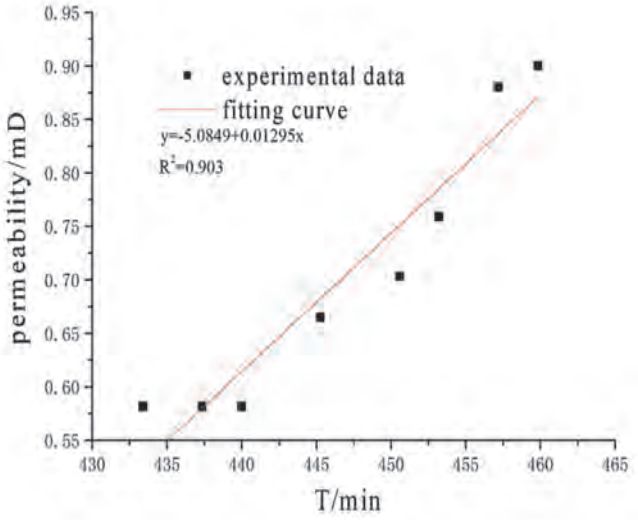

(a) Confining pressure, 2 MPa and gas pressure, 1 MPa

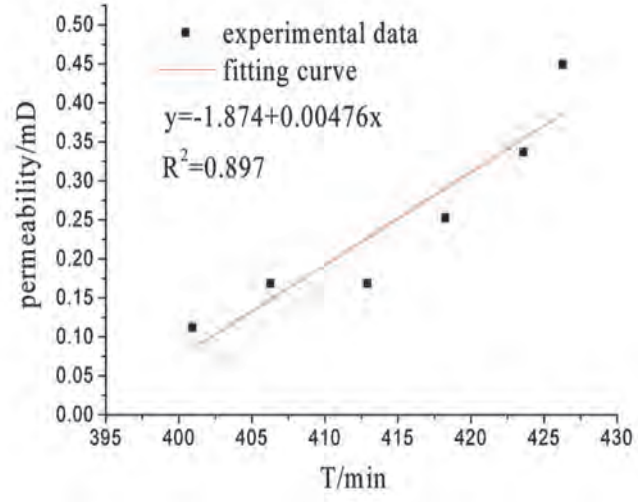

(b) Confining pressure, 6 MPa and gas pressure, 1.6 MPa

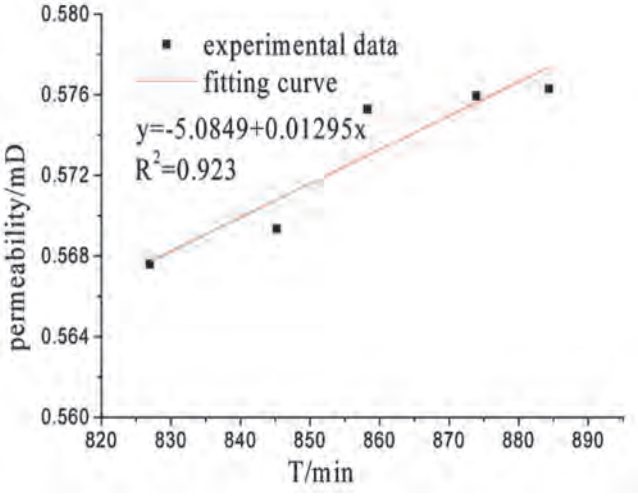

(c) Confining pressure, 8 MPa and gas pressure, 1 MPa

Fig.7 Evolution of permeability in the steady creep stage under failure stresses

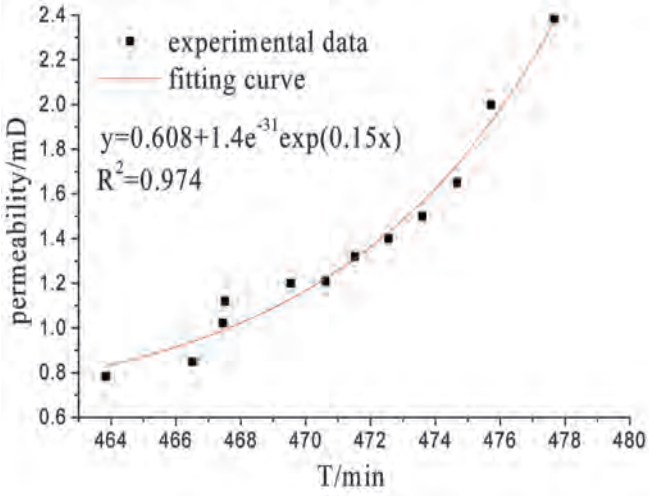

(a) Axial pressure, 30 MPa, confining pressure, 2 MPa, and gas pressure, 1 MPa

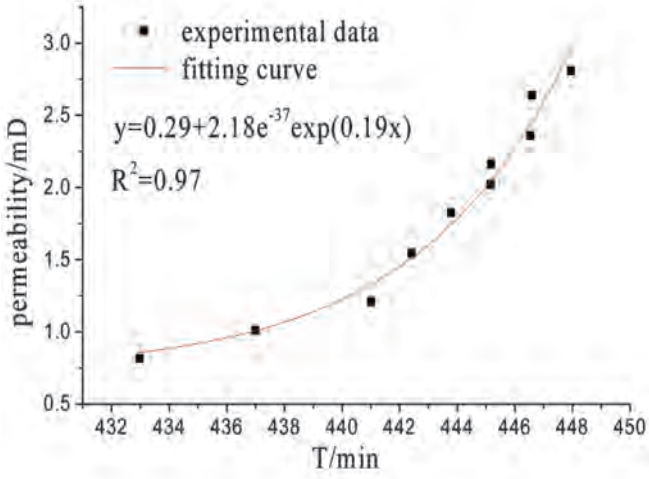

(b) Axial pressure, 62 MPa, confining pressure, 6 MPa, and gas pressure, 1.6 MPa

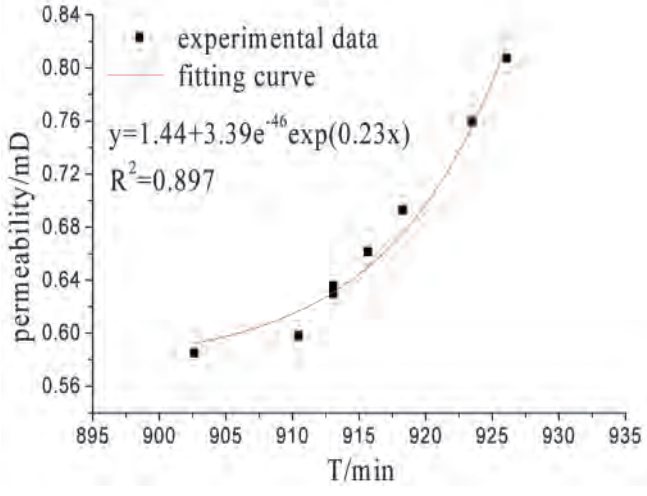

(c) Axial pressure, 84 MPa, confining pressure, 8 MPa, and gas pressure, 1 MPa

Fig.8 Evolution of permeability in the accelerated creep stage under failure stresses

(a) 1-1 (b) 1-3 (c) 1-4

Fig.9 Failure of the coal samples under multi-stage loading

tendency of plastic flow in the deformation process to occur with increasing confining pressures.

It can be seen from experimental data that permeability evolution of the coal samples in the three creep stages under failure stress was consistent with the axial deformation of the coal samples. From the volumetric deformation, it can be seen that permeability of the expanded coal samples grew to some extent, which was the result of fracture evolution within the coal samples. Fundamentally, extension and connection of fractures inside the coal samples played a dominant role in the evolution of their permeability. On the whole, the permeability decreased because of the closure of pores and fractures during compression as external loads increased, then the fractures appearing inside the coal samples formed effective passages allowing gas transport, which was the primary reason for the observed increases in permeability. Macro-fractures, formed after the failure process had started, caused sudden changes in the permeability, but as the coal samples were still subjected to triaxial compression, buckling failure did not occur.

4.3 Relationship between coal permeability and volumetric strain

It can be seen from the images of the failed sample they had dilated: experimental data showed that there was a correlation between volumetric strain and permeability. During creep testing, the axial pressures and confining pressures remained unchanged while the strain increased with time, which corresponded to the slowly increasing permeability seen after the onset of significant dilatation. In addition, the evolution of permeability showed a direct relationship to the strain state. By reorganising the experimental data under failure stresses during the creep stage, relationships between permeability and volumetric strain (under failure stresses) were obtained, as shown in Fig.10.

Fig.10 shows that the permeability of the coal samples during creep increased with increasing volumetric dilatation.

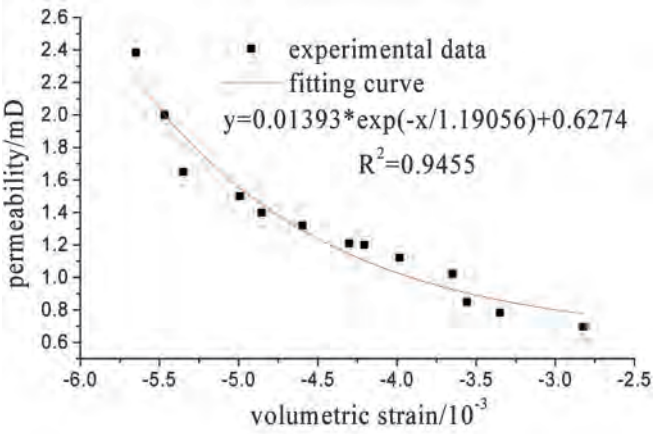

(a) Axial pressure, 30 MPa, confining pressure, 2 MPa, and gas pressure, 1 MPa

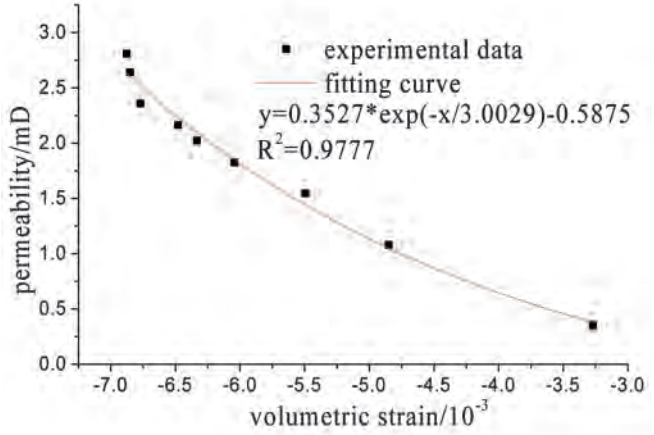

(b) Axial pressure, 62 MPa, confining pressure, 6 MPa, and gas pressure, 1.6 MPa

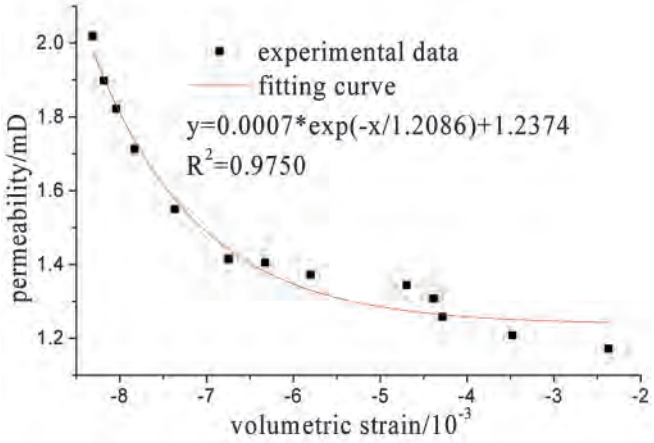

(c) Axial pressure, 84 MPa, confining pressure, 8 MPa, and gas pressure, 1 MPa

Fig.10 Relationships between volumetric strain and permeability under failure stresses

In the first two stages, the volumes of the coal samples changed to some extent but the permeability underwent less of a change. In the accelerated stage, the volumetric deformation increased significantly, as did the permeability which became several

Table 2: Permeabilities in different creep stages under failure stresses

Axial pressure / MPa	Confining pressure / MPa	Gas pressure / MPa	k_1 / mD	k_2 / mD	k_3 / mD	k_4 / mD
30	2	1	0.5853	0.5817	0.7830	2.3845
62	6	1.6	0.5036	0.1123	0.8146	2.809
84	8	1	0.5810	0.5676	0.5849	0.8074

Note: k_1, k_2 and k_3 represent initial permeabilities in the attenuated creep stage, steady stage, and accelerated creep stage, respectively; k denotes the permeability of the coal samples at failure

times, even several tens of times, greater than the initial permeability in the steady creep stage. Combining this finding with the experimental data, it can be seen that evolutions of both permeability and volumetric strain were similar and volume change was an important factor affecting the evolution of the permeability. Data fitting showed that, in the creep failure stage, the changes in permeability and volumetric strain followed an exponential function, as shown in Formula (2):

$$k = a\exp(\varepsilon_v / b) + c \quad \ldots \quad (2)$$

where, k represents the permeability of the coal sample, a, b, and care fitting parameters, and ε_v is the volumetric strain.

5. Conclusions

The seepage from coal samples collected from the No. 3 coal seam of Rundong coal mine was tested during imposed creep strain and various triaxial stress states to study the evolution of the permeability therein. Based on the experimental results, the following results were obtained.

(1) Obvious attenuation creep deformation and static deformation appeared during the creep process caused by multi-stage loading under low stress, and the permeability decreased during the loading process and creep stage. The permeability decreased rapidly during the initial stage, gradually reaching a stable value and then, it changed in a sense opposite to the changes in axial deformation. Moreover, high confining pressures exerted certain inhibiting effects on permeability evolution in these coal samples.

(2) The permeability varied slightly in the attenuated, and steady, stages under creep and at sample failure stresses, it decreased in the attenuated creep stage, while it increased linearly in the steady stage. In the acceleration stage, the permeability increased significantly to a value that was several times larger than the initial permeability in the steady creep stage when the coal body was first damaged.

(3) In the creep damage stage, the changes in permeability and volumetric strain followed an exponential relationship.

Acknowledgment

This work was supported by the National Natural Science Foundation of China (NSFC) (Grant no. 51174082 and51604091); the Key Scientific Research Projects in the Colleges and Universities of Henan(Grant no. 17A440002);and Doctoral fund of henan institute of engineering(Grant no.D2017001).

References

1. Xu, J., Peng, S. G., Tao, Y. Q. and Yang, H. W. (2009): "Experimental analysis of influence of creep on permeability of gas bearing coal," *Chin J Rock Mech Eng*, vol. 28, no. 11, pp.2273-2279, 2009.
2. Ying, G. Z., Zhang, D. M. and He, X. G. (2009): "Creep experiment and theoretical model of gas-containing coal," *Chin J Geo Eng*, vol. 31, no. 4, pp. 528-532, 2009.
3. Wang, D. K., Liu, J., Yin, G. Z. and Wei, X. J. (2010): "Test study of creep properties of gas bearing coal specimens under triaxial compression," *Chin J Rock Mech Eng*, vol. 29, no. 2, pp. 349-357, 2010.
4. He, F., Wang, L. G., Wang, Z. W. and Yan, Z. X. "Experimental study on creep-seepage coupling law of coal (rock)," *J Chin Coal Society*, vol. 36, no. 6, pp. 930-933, 2011.
5. Wang, R. B., Xu, W. Y., Wang, W., Zhang, Zh. L. and Zhang, Y. (2010): "Experimental investigation on creep behaviors of hard rock in dam founfation and its seepage laws during complete process of rock creep," *Chin J Rock Mech Eng*, vol. 29, no. 5, pp. 960-969, 2010.
6. Wei, J., Wang, Y. Y., Qi, J. and Li, J. G. (2011): "Mathematical model of seepage in porous medium on account of solid-fluid coupling and creep effect," *J L N Tench Univ (N S)*, vol. 30, no. 5, pp. 726-729, 2011.
7. Guo, B. H. and Tian, C. X. (2012): "Normal creep deformation law of rock fracture and the influence of seepage," *J H N Polytech Univ (N S)*, vol. 31, no. 4, pp. 403-408, 2012.
8. Cao, Y. J., Wang, W., Xu, W. Y., Wang, R. B. and Wang, H. L. (2015): "Permeability evolution of low-permeability rocks in triaxial creep tests," *Chin J Rock Mech Eng*, vol. 34, no. S2, pp. 3823-3829, 2015.
9. Chen, J. G., Liu, W. Q. and Liang, H. N. (2015): "Creep-seepage coupled Analysis of Underground fractured rock mass," *J Yangtze River Scienti ResecrInstit*, vol. 32, no. 11, pp. 45-51, 2015.
10. Dai, Z. X. and Lv, Y. C. H. (2015): "Seepage experiment of sandstone during creep processes," *Chin Mining Magaz*, vol. 24, no. 7, pp. 329-332, 2015.
11. Zhang, Y., Xu, W. Y., Zhao, H. H., Wang, W. and Hao, J. F. (2014): "Experimental investigation on permeability evolution of sandstone from fractured zone under coupling action of hydro-mechanical-creep," *J China Univ Petro*, vol. 38, no. 4, pp. 154-161, 2014.
12. Yang, H. W., Xu, J., Nie, W. and Peng, S. J. (2015): "Experimental study on creep of rocks under step loading of seepage pressure," *Chin J Geotech Eng*, vol. 37, no. 9, pp. 1641-1649, 2015.
13. Tian, K. Y. and Zhang, R. L. (2014): "Research on triaxial stress seepage experiment device loaded by high pressure water and negative pressure," *Rock & Soil Mech*, vol. 35, no. 11, pp. 3338-3343, 2014.